Supportive Robotic Welding System for Heavy, Small Series Production with Non-Uniform Welding Grooves

Csongor Márk Horváth, Péter Korondi

Department of Mechatronics, Optics and Mechanical Engineering Informatics, Faculty of Mechanical Engineering, Budapest University of Technology and Economics, Műegyetem rakpart 1, 1111 Budapest, Hungary
hcsongorm@mogi.bme.hu, korondi@mogi.bme.hu

Abstract: Heavy welding is a demanding task with high robotization potential. This applies especially for the runners of Francis hydropower turbines, due to the high working costs and EHS requirements in Europe. However, heavy welding is often related to small-series production with long processing time. This sets high demands on the planning and monitoring functionality of the robot system. The research in this field is gaining momentum, yet very few articles suggest suitable solutions. This paper presents a robotic welding control system design and application that facilitates the planning, control, and monitoring of the welding process of non-uniform grooves of large-dimension joints. Its primary and unique characteristic is the simplified operator assisted programming method, where the three-dimensional path modification problem is translated into consecutive two-dimensional modifications. Therefore, reference cross-sections are created along the welding groove, where the sequence planning task of multi-pass weld bead placement is performed, and to the online modifications together with the adjustments are referred. The planning, changes and process supervision are supported by the robot system to handle uncertainties along the welding groove and adaptively utilize the robot operator experience. The activities are tracked and organized to supply information for later performance enhancement and reusability between similar processes. The supportive system design is particularly suitable for advanced, large-dimension, heavy robotic welding applications. A use case is presented on a welding a runner of Francis hydropower turbine.

Keywords: robotic welding; multi-pass welding; non-uniform groove; small series production

1 Introduction

1.1 Welding Robots for Small and Medium Sized Companies

The industry is facing major challenges increasing efficiency and productivity to stay competitive. The small and medium sized enterprises (SMEs) are an essential part of the countries' economy, as they represent 99 per cent of all enterprises. The domain of industrial robot usage and integration has been dominated by the large-scale automotive and electronics industries [19, 30]. With 27%, the automotive sector is the largest in the welding industry. From all application fields, the most common is welding and soldering (30%), which typically implemented for large volume production that requires high product mix and short production cycle. Although recent trends show an expansion of robot adoption outside of these areas, the progression into new fields is moderate.

Even though the SMEs are showing increasing demand for robotization, their demands differ from the traditional robot applications because their business models are more likely to involve wide range and small series production [26]. The tasks are often not well defined, heavy, fatiguing and hazardous, with substantial environmental load and stress level for the workers [35]. The limited proof of performance of the technologies are the technical barriers that limit the adoption of robotic systems by SMEs even in the most desired application areas.

Despite the quality and efficiency that a today's robotic welding systems can provide for the general welding industry, skilled human welders cannot yet be replaced in welding of joints in complex structures due to various reasons: high initial costs, tedious teaching procedure and long commissioning time. Thus, most of the welding is done manually or semi-automatically in fields such as the offshore industry, ship manufacturing or hydropower turbine production [17].

1.2 Challenges in Heavy Multi-Pass Welding

Several challenges arise when the application comes to robotic heavy welding despite the convenience of using robotic welding systems. Typical challenges related to the small series production are the following:

1. Cost and personnel: SMEs have limited resources; The high initial costs of installations with the lack of dedicated and specialized personnel restrict the possibilities to deploy robotized solutions as well as the use of complex offline programming systems at SMEs facilities.
2. Task complexity: Large-dimension welding joints typically have thick and non-uniform welding grooves. Therefore, significant amount of time and so-

phisticated approach are necessary to handle the multi-pass welding process. Such grooves are often still welded manually due to their complex shape.

3. Environment: The heavy, fatiguing and hazardous manual welding, with substantial environmental load and stress level for the workers effects directly the production and need to be conformed with the Environmental and health (EHS) regulations

4. Programming time: Small series production requires significant effort spent on the programming of the welding robot for the new part. The currently available robotic solutions are lacking a detailed model based multi-pass welding planning. An accurate multi-pass welding plan can shorten the preparation and welding time.

5. Handle uncertainties: Robots cannot make corrective decisions autonomously. Thus, decision making support is required, either by the sensors and the control system or through intuitive user interaction. Detailed and accurate knowledge about the process increase the applicability range of the planning, but, additional online handling of the arising uncertainties is inevitable.

The welding groove complexity of large-dimension joints originates mainly from the geometry and the varied thickness of the base materials. Regardless of the careful edge preparation and the standard conformity, weld joints have thick non-uniform grooves. Such examples are the tubular joints in pipeline manufacturing or the grooves on the hydropower turbine runners at the blades.

This paper presents a robotic welding control system design and application that facilitates the planning, control, and monitoring of the welding process of non-uniform grooves. Its primary and unique characteristic is the simplified operator assisted programming method. It contains an offline programming module with dedicated consideration of the non-uniformities of the welding groove and the simplified online programming module, supporting the welding path adjustment and process supervision to handle uncertainties. The supportive system design is presented on a use case with a runner of Francis hydropower turbine.

2 Background

2.1 Welding Robot Systems

Welding robots represent the largest fraction of applications deploying industrial manipulators. The most common techniques apply Metal Inert/Active Gas welding (MIG/MAG), the Tungsten Inert Gas (TIG), and Laser Beam Welding. Currently, automated robotic welding is gaining momentum due to the high wage levels and the dropping installation and operation cost of a robot system. This offers new opportunities to automate small series production, although these are the result of several stages of development in the welding robot systems.

In the earliest, first generation robotic welding applications, the welding was performed in two runs; the first run was dedicated to learning the seam geometry and the second run was the actual tracking and welding. The second generation of robotic welding systems' development reduced the number of necessary runs by performing seam learning and tracking simultaneously, in real-time. The latest, third-generation welding robot systems are not only operated in real-time but within unstructured environments and learning the rapidly changing geometry of the seam during operation [36].

According to Pires [36], an automated robotic welding system design can be implemented in three different phases with the final goal to achieve decent performance and a high-quality weld. The first phase is the preparation, where the welding scene is set up and the offline programming is executed. The second phase is the welding phase, when the welding process is performed based on the continuous decisions made by the operator or the robot system to achieve the required weld quality. The last phase is the analysis phase, in which the welds are examined, and a decision made about the acceptance. The considered changes are collected and evaluated.

2.2 Hardware Components

Modern welding robot systems contain an integration of the robot manipulator, robot controller, welding equipment, work-piece positioner, supportive sensor system, and welding safety devices [12,31]. Those multiple units require coordinated or synchronized motion to access the entire work-piece, minimize idle time and maximize the arc/welding time. It often connected to a sensor system supporting the welding process and a computer for process control and data collection. In advanced operations, the standard computer peripheries are extended by additional Human-Machine Interfaces (HMI). A schematic of a general robot system is shown in Figure 1. Similar equipment used for the realization of the robotic welding system presented in this paper.

Sensors in robotic welding are used to detect and measure process features along with geometrical parameters, or monitor and control welding process parameters by technological sensors [13, 21, 48]. The first can be achieved in several ways applying most often optical sensors to detect and measure the joint geometry (seam finding, seam tracking) [49, 50], as well as the weld pool geometry and location [9, 37]. Research on robot systems for small series production has been conducted to determine the main factors for the users. Besides the flexibility, user-friendliness, shorter programming time, and robustness of operation, the possibility to integrate sensors both for simulation and during runtime was listed as significant. In this context, sensors used for seam tracking or to control the welding process are considered equally important [3]. Weld quality monitoring in robotic welding provides automatic detection of weld defects by analysing the process parameters and by comparing these with the nominal values [38]. It also could include non-destructive inspection methods such as radiography, ultrasonic, vision, magnetic detection, eddy current, acoustic measurements [55] or electromagnetic sensor [1].

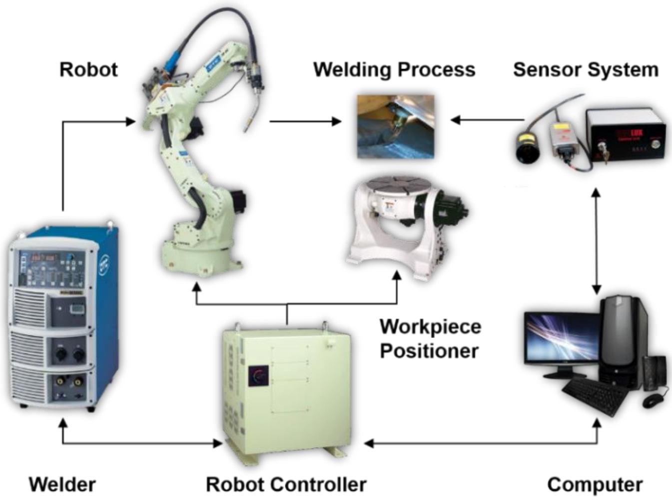

Figure 1
General robotic welding system

Due to the challenging formation of the high temperature welding environment (high current, spatter, liquid metal, high temperature), it is difficult to apply sensors to measure the welding parameters directly. These problems cause that the parameters that can be observed are not concurring with the parameters needed to be controlled. Furthermore, it is not trivial to carry out a simple feedback control. The complexity can be solved by developing models to map the observable parameters to appropriate actions on issues within the relevancy of the welding specification procedure. In this, the productivity and quality measures are defined together with the nominal welding process control parameters and geometry information to produce the desired weld. A model based control should, therefore, unify the data from the sensors, the welding procedure specifications and the robotic welding system specific restrictions [36].

2.3 Programming Methods

Two main categories of programming methods exist in practical industrial applications: online programming, including the lead-through and walk-through, and offline programming (OLP). Conventional online programming allows for precise control of the straightforward process with simple path definitions and work-piece geometry. Due to the low initial cost and low programming skills required, it is widely used. However, the entire production line is disrupted during teaching due to the downtime of the robot. Moreover, the taught program has limited flexibility and is unable to adapt to the current welding scenario and problems encountered in the welding operation without additional control [34].

More advanced programming methods are the operator-assisted online programming, such as the lead- and walk-through methods or the sensor guided programming. By walk-through programming, the robot arm itself is configured to be able to be moved by the operator, to teach the robot path based on the built-in [2, 7, 42] or external sensors [41]. Furthermore, experiments and research have been conducted to develop admittance controller driven teaching methods, deploying external tools [27, 44] and vision systems [33, 43, 45]. Besides the progress achieved on the online programming to make it more intuitive and fitting of the operator skills, most of the research outcomes are still not commercially available [34].

Using OLP methods, data based on CAD/CAM is a common practice in many areas of the industry, especially automation systems with large product volumes. Figure 2 illustrates the workflow of OLP. Many software and simulation tools are available to provide direct robot trajectories from CAD data of the work-pieces, robots, and fixtures used in the cell [20]. Some of the most advanced techniques apply the recent results of research in the field of Cyber-Physical Systems [10, 29, 39] and the Digital Twin [32, 46] related developments. The main advantages are that the generated code is reusable, flexible for modifications, and complex paths can be produced with reduced production downtime [18]. However, the OLP systems utilization in SMEs is limited due to the economic disadvantages for small volume production caused by the high cost of the OLP packages and the programming overhead for customization [34].

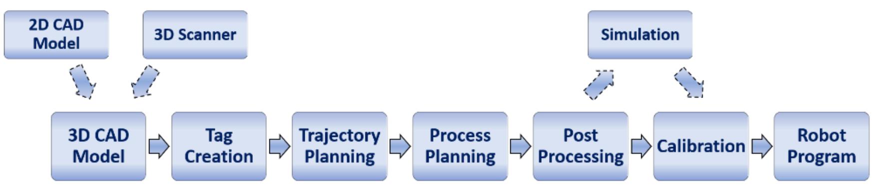

Figure 2

Key steps of offline programming. Reprinted from [34]

In welding, most of the available OLP software is considering the welding seam as a well-defined, uniform groove. The existing planning methods of multi-pass welding [25, 52, 53] based on a generally constant grove cross-sectional area where the differences in the geometry are results of errors. Only a few studies [6, 51] analysed how to handle the non-uniformity of the welding groove geometry systematically. These address the groove representation with straight edges, where the measured profile showed different shape, without consideration of the curvature of the edge preparation. The layer height calculation was based on trigonometrical principles. The introduced welding groove segmentation based on the weld bead placement strategy and the welding position difference. The groove geometry changes affected the weld bead numbers in the layers and the number of the layer number. One of the main conclusions was that the weld bead number in the layers should be constant, but the layer number would vary from segment to segment concerning the welding quality.

2.5 Human Behaviour Models and Human-Machine Interfaces

The mainstream trend in modern welding industry is mechanization and automation. However, human welders may be preferred over mechanized welding control systems in applications where experience-based behaviour in response to the received information is required [54]. Studies have been conducted to develop models of the mechanism of welders' experience-based behaviour to create a controller in automated welding. It has been found, that the welder makes decisions primarily based on past learned experiences and the humanistic approach of the acquired sensory information is imprecise. It only reflects partial truth about the instant status of the welding process [5, 23].

Another approach is to create HMI to overcome the barriers between the process and the operator, by improving the maintenance and support activities through remote communication [4]. This can be exploited by cyber-physical devices [8], cognitive info-communication methods [16, 22], or multi-modal man-machine communication (4MC) [28, 47]. Those latter methods utilize multiple senses of the human and create sensor bridging to transfer the otherwise naturally acquired data (NAD) [22]. Information from one sensor must be translated into another and transferred through non-conventional communication channels (Figure 3). Therefore, the goal of multi-modal human-machine communication is to realize natural, intuitive and efficient information flow between the remote operator and the local system [47] as well as create a virtual environment that makes the remote operator feeling next to the system [11, 14, 15, 24].

Based on the overviewed literature, the guidelines can be identified for the development of a heavy multi-pass welding robot system for SMEs. Cost and time efficient programming method is required to provide alternatives to the expensive and general OLP methods along with the slow but flexible online programming.

The development of a simplified OLP system is defined to achieve the necessary complexity level by automating the auxiliary, non-welding tasks; simplify online programming by developing HMI for the execution of the essential modifications integrated it into the control system. The sensor system must be integrated to support the operator's modification activity.

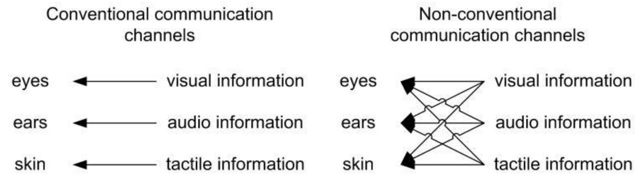

Figure 3

Differences between conventional and non-conventional information channels [16]

The simplified and process-oriented environment could balance out the missing skill set of the robot operator, and the supportive sensory system provides the necessary information to utilize the operator experience in welding.

3 Control System Structure for Heavy, Multi-Pass Robotic welding

This section provides a general description of the system design principles for welding tasks with large-dimension joints and non-uniform grooves. The system design is intended to replace the manual welding procedure directly, but it also needs to be able to compete with the online and offline programming methods. Figure 4 provides the schematic for such a system that can be considered as a cascade control system design. This contains three different control loops with different speed and functions, furthermore divided into the phases discussed in Section 2.1. The process consists of the preparation, offline planning and programming, the welding process control, and finally the observation and analysis.

3.1 Preparation and Offline Programming

The process starts with the welding scene setup, where the preparation includes the work-piece positioning, the welding method and the additional physical components definition (shielding gas, feed wire, preheating). The outermost loop of the cascade control system is offline programming and analysis loop, which performed between the different welding setups. Its forward section contains the offline programming, where the CAD/CAM models are handled. Based on the planning strategy of multi-pass welding and the weld bead models, the weld seam is filled, and the robot trajectory is generated according to the calibration procedure. The feedback section includes the post weld analysis and the learning to update the planner algorithms for further applications.

The welding joint defined in the CAD model of the work-piece with the given groove geometry and the root weld path. Along this path, two-dimensional cross-sections can be extracted from the model that followed by multi-pass weld bead placement planning applied for each cross-section individually. A sectioning algorithm creates sections along the groove to create a unified weld bead pattern for the segment. The planning phase is closed by the trajectory generation in the model space that translated into robot trajectories after work-piece calibration. The direct paths transferred to the robot controller, where they become executable.

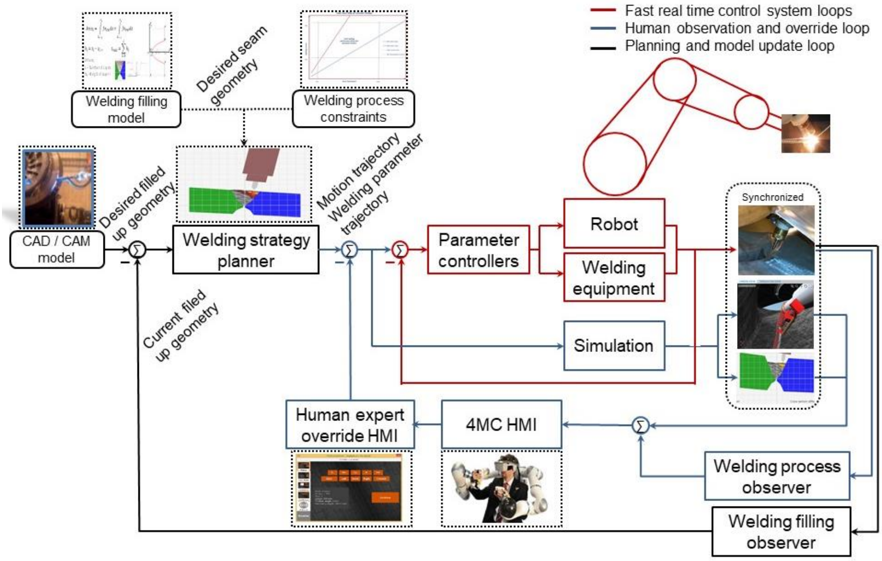

Figure 4

Scheme of the welding robot system

3.2 Welding Process Control

The inner part of the process structure is covering the welding phase with two overlapping control loops. The most inner loop represents the real-time control system of the welding process and the robot motion controlled by the robot controller. The feedback contains the robot system and welding process variables, such as the recent tool position for motion control and the measured values for the welding parameters.

The middle loop is the human interaction loop where the adaption is performed to the immediate situation during the welding process or to the desired path during the path setup and verification. Here, the feedback loop includes the observations of the welding process and the correction actions from the operator. On the given user interface, the cell operator could give commands to the system to perform the predefined sub-tasks that includes the path verifications and the welding executing. Furthermore, it offers path adjustments both during the dry-run and the weld-run.

3.3 Observation and Post-Weld Analysis

The post-weld analysis and observation are performed to validate the welding process goodness and decide about the acceptance or detect the defects of the welding. The proposed system is intended to handle all the available information collected during the preparation and the welding process, including the synchronized data gathered from the robot controller (speed, position and orientation information, input and output values, internal variable values), from the welding power source (variable welding parameters, pre-set welding parameters), and from the cameras and sensors. The data collection extended with the weld qualification measurements (visual inspection, destructive and non-destructive examination methods) can provide the information needed for a well-supported decision to adjust the reference parameters for the future welding processes.

4 Offline Programming and Path Verification

The programming of the robot and the verification of the welding path are linked together, and the proposed system supports this process with minimal user interaction. Figure 5 shows how the same path is represented in the different scenarios: first in the path definition phase, then in simulation, finally the path verification. This section provides descriptions about the offline programming system, including the transformation chain from the predefined machining path definition in model space to executable robot trajectory.

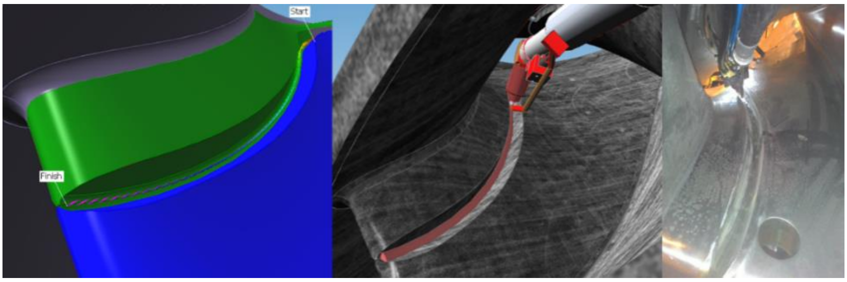

Figure 5
Root welding path verification utilizing a digital twin

4.1 Root Weld Path Definition and Reference Cross-Sections

The root weld path is defined during the offline programming and preparation phase and serves later as a reference trajectory of the multi-pass welding planning. The offline programming tool reads the CAD file of the work-piece then the groove definition is given including the reference cross-sections and the root weld path. The root weld path is built up from task points and normal vectors where the distribution and density of the points define the resolution of the path on the necessary level (straight grooves requires fewer control points compared to curvy grooves) and the normal vectors determining the initial welding torch orientation as shown in Figure 6. The schematic representation of the coordinate system and vector definitions are given in Figure 7. The reference coordinate system for the CAD/CAM data is defined as ***r***, the robot's base coordinate system is defined as ***b***.

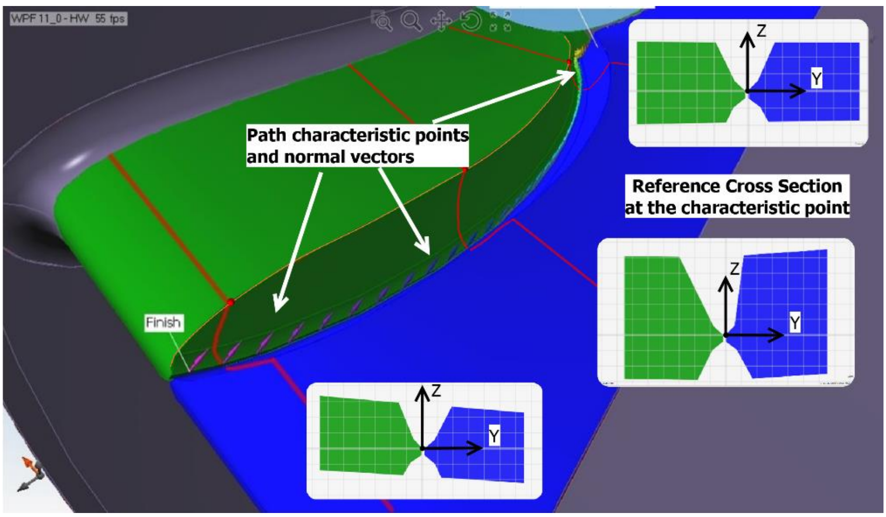

Figure 6

Root weld path trajectory definition in the model space as the digital representation of the work-piece

The task point coordinates $\underline{C}$ are defined in the model $\mathbf{r}$ coordinates and given in the path definition description with the path normal vector $\boldsymbol{a}$, which is a physical reference for the initial welding torch orientation. The tangent vector of the path $\boldsymbol{n}$ is targeting the next task point respecting the predefined task direction. The third vector at the task point $\boldsymbol{s}$ is the cross product of the $\boldsymbol{a}$ and $\boldsymbol{n}$. The task path description in the reference $\boldsymbol{r}$ model space coordinated system is denoted as $\{\boldsymbol{T_C}\}^r$ that includes each task points and their local coordinate system definition and provides the basis for the robot trajectory planning.

Reference cross-sections are generated from the CAD model along the root weld path to reduce the complexity of the path adjustments and to be used later during the multi-pass welding planning phase. The cross-sections are perpendicular to the path trajectory and defined for each task point on the plane of the local coordinate system $\boldsymbol{t}$, represented by the two vectors $\boldsymbol{a}$ and $\boldsymbol{s}$, where vector $\boldsymbol{a}$ defines the z-axis and vector $\boldsymbol{s}$ defines the y-axis. The process of the transformation steps and matrixes is shown in Figure 8. and described in detail in the following.

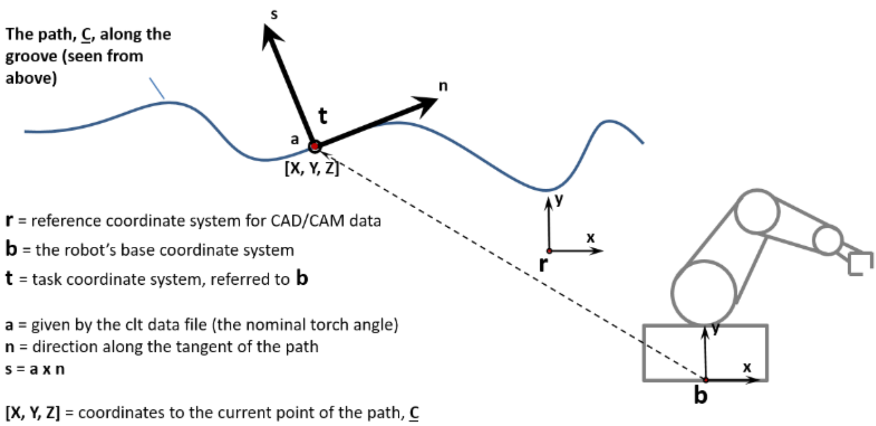

Figure 7

Definition of the reference coordinate systems

$$\boldsymbol{CLT} \to \{\boldsymbol{T_C}\}^r \Rightarrow \{\boldsymbol{T_C}\}^b = \boldsymbol{T}_r^b \times \{\boldsymbol{T_C}\}^r \Rightarrow \{\boldsymbol{T'_C}\}^b = \{\boldsymbol{T_C}\}^b \times \Delta\boldsymbol{p}^t \Rightarrow \{\boldsymbol{T''_C}\}^b = \{\boldsymbol{T'_C}\}^b \times \Delta\boldsymbol{r}^{t'} \Rightarrow \{\boldsymbol{T'''_C}\}^b = \{\boldsymbol{T''_C}\}^b \times \{\widetilde{\Delta c}\}^{t''}$$

Figure 8

Structure of coordinate transformation – from CAD to executable motion trajectory

4.2 Welding Process Planning

The central part of the process planning in offline programming is the definition of the multi-pass weld bead pattern and the corresponding robot trajectory definition. During the multi-pass welding planning, the main controllable online variable settings collected for each weld bead that influences the welding process, namely arc voltage, arc current, torch travel speed, and wire feed rate. The welding parameters range is defined in the Welding Procedure Specifications as constraints for all weld bead related planning and modelling.

The commercially available welding systems do not contain model-based planning capability considering the weld bead profile properties. Such modules often only generate a symmetric and simplified weld bead layout, which usually requires major adjustments during the operation. In this proposed method, the positions of the weld beads are defined based on certain placement strategies and based on consideration of the groove geometry and the model of the weld bead profile function. Further plan-specific parameters are also included, such as the length of the seams, the welding torch orientation and collision avoidance modifications. The block diagram of the planning process is presented in Figure 9.

The planning process starts with the groove modelling (Block A1), when the groove's mathematical description made for each characteristic cross-section from the digital representation of the work-piece and the weld groove (CAD/CAM or profile scan data as I1-I3). The next step is the generation of the initial weld bead placement sequence in each given groove cross-sections handled by the Sequence Planner (Block A2). The weld bead sizes, shapes and welding parameters are defined by the Welding Filling Model (C1).

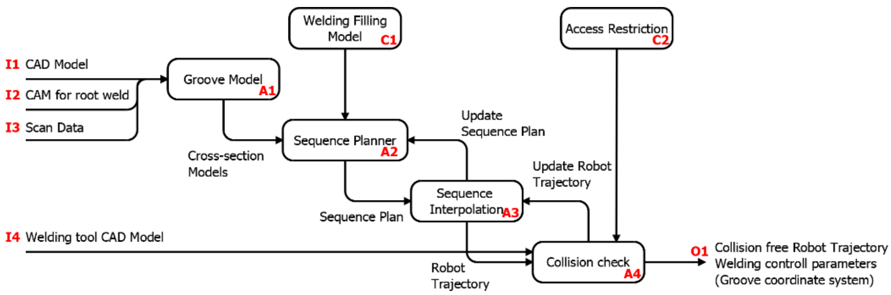

Figure 9

Planning process of multi-pass welding

The model uniqueness lays in the realistic representation of the weld bead profile function in the layer-by-layer deposition, instead of the conventional quadrilateral approximation, described by Yan, et al. [51]. The weld bead shapes are described as symmetric curve functions, and the edge preparation of the grooves defined as continuous convex functions. The produced ripple top surface of the layers is better suited to reality than the flat surface approximations, therefore, the cumulating error is significantly reduced during the deposition. The exact implementation of the Welding Filling Model and the representation model of the weld bead profile is not synergic part of this paper. When the pattern is generated, the Sequence Interpolation section (Block A3) is activated to assure the pattern smoothness, creating sections for a consistent plan and starting the new iteration process to apply a generally accepted plan. This generates the initial robot trajectories with connected welding parameter settings. The last step (Block A4) is to adjust the recently created robot trajectories concerning the confined space access restriction, to avoid collisions.

4.3 Calibration and Path Definition

The trajectories generated by the multi-pass welding planner are referred to the local coordinate system in the model space but need to be transferred to the robot coordinate system before executions by coinciding with the location of the physical work-piece and the CAD model. This is done by performing a calibration procedure, through determining the position of the same reference coordinate system on the physical work-piece as being used in the virtual world where the CAD / CAM model is defined. During the calibration procedure, the $\boldsymbol{T}_{\boldsymbol{r}}^{\boldsymbol{b}}$ transformation matrix determines the translation and rotation from the model space $\boldsymbol{r}$ coordinate system to the robot's base coordinate system $\boldsymbol{b}$. resulting the new coordinate definition as $\{\boldsymbol{T}_C\}^b$, according to Equation 1.

$$\{\boldsymbol{T}_C\}^{\boldsymbol{b}} = \boldsymbol{T}_{\boldsymbol{r}}^{\boldsymbol{b}} \times \{\boldsymbol{T}_C\}^r \qquad (1)$$

5 Online Process Control

By the end of the offline programming and process planning, the input parameters are available for the online process control that is the primary process in the welding phase [40]. The input parameters are the motion trajectory and the welding parameter trajectory. In this section, the block of the online process control is discussed (Figure 4). It includes the control of the physical robot system with the connected devices, the digital twin which is running parallel to the welding process, the welding process observer, which is acquiring the information about the process, and the human-in-the-loop.

The process flow can be described as the following: The reference motion trajectory and welding parameter trajectory are transferred to the parameter controllers. Those reference values translate into executable parameter sets and sections communicated to the physical devices (robot controller and welding power source). The physical signals feedback to the parameter controllers providing stable signals to the welding process. The control loop implementation is distributed between the physical devices including the factory designed parameter controls. This parameter control with the devices is the most inner loop of the cascade control system. The digital twin is running parallel to this loop including the digital representations of the devices and the work-piece.

The welding process observer is the feedback of the welding process, including the supportive sensor system and overlapped with the information gained from the digital twin. Practically, the latter provides information about the hardly observable parameters, such as the current cross-sections, the already and the future deposited weld beads' reference torch position, as well as collision alerts. The feedback loop includes the human operator, for whom the information is translated through 4MC devices and if necessary overwrites the process references.

5.1 Applying Path Modifications: Translation and Rotation

Our approach to applying path modifications in the welding process is to separate the translation modifications from the rotations. Thus, the three-dimensional path modification problem is translated into consecutive two-dimensional modifications, where the reference cross-sections are serving as a modification plane. The reference cross-sections remain constant during the process regardless of the applied path modifications. The multi-pass welding planning becomes trackable for the operator. The user translation modifications are given along the reference cross-sections main axes as Δy and Δz, relative to $\boldsymbol{t}$ task point. The new point $\boldsymbol{t'}$ is the result of the translation $\Delta\boldsymbol{p^t}$ defined by $\{\boldsymbol{T'_C}\}^{\boldsymbol{b}}$ as shown in Equations 2.

$$\{\boldsymbol{T'_C}\}^{\boldsymbol{b}} = \{\boldsymbol{T_C}\}^{\boldsymbol{b}} \times \Delta\boldsymbol{p^t} \tag{2}$$

The user rotations $\Delta\boldsymbol{R_{x,\varphi}}$ and $\Delta\boldsymbol{R_{y,\theta}}$ are applied to the translated point $\boldsymbol{t'}$, the transformation is combined as $\Delta\boldsymbol{r^{t'}}$ and is applied to resulting the new orientation transformation $\{\boldsymbol{T''_C}\}^{\boldsymbol{b}}$ at the task point, according to Equation 3 and 4. The physical meaning of those transformations is that the $\Delta\boldsymbol{R_{x,\varphi}}$ defines the rotation of working angle of the torch by φ, the $\Delta\boldsymbol{R_{y,\theta}}$ defines the rotation of the travel angle by θ. Rotation around the path tangent vector (x-axis) is applied when the penetration on the groove face needs to be increased by asymmetrical heat distribution.

$$\Delta\boldsymbol{r^{t'}} = \Delta\boldsymbol{R_{x,\varphi}} \times \Delta\boldsymbol{R_{y,\theta}} \tag{3}$$

$$\{\boldsymbol{T''_C}\}^{\boldsymbol{b}} = \{\boldsymbol{T'_C}\}^{\boldsymbol{b}} \times \Delta\boldsymbol{r^{t'}} \tag{4}$$

Both, the translation and rotation modifications made by the operator can be applied to refine the predefined paths on the multi-pass welding plan to increase its accuracy and provide processed data for further analysis to enhance the planning.

5.2 Collision Avoidance and the Final Combined Transformation

In the confined working area, the final path transformation should be made to avoid collisions. The rotations are applied in the reference coordinate system $\boldsymbol{r}$ along the vectors $\boldsymbol{a}$ and $\boldsymbol{n}$. The resulting transformation matrix is denoted by $\Delta\boldsymbol{c}^{\boldsymbol{r}}$ as the cross product of rotation $\Delta\boldsymbol{R}_{\boldsymbol{y},\boldsymbol{\theta}}$ (around $\boldsymbol{a}$) and $\Delta\boldsymbol{R}_{\boldsymbol{z},\,\boldsymbol{\psi}}$ (around $\boldsymbol{n}$) (Equation 5). However, the $\Delta\boldsymbol{c}^{\boldsymbol{r}}$ transformation should first change its base from $\boldsymbol{r}$ to $\boldsymbol{t}''$, therefore, Equation 6 should be applied to calculate $\Delta\boldsymbol{c}_{\boldsymbol{i}}^{\boldsymbol{t}''}$. Introducing maximum limit for angle change in the collision avoidance $\Delta\boldsymbol{R}_{\boldsymbol{z},\,\boldsymbol{\psi}_{\boldsymbol{max}}}$ and $\Delta\boldsymbol{R}_{\boldsymbol{y},\boldsymbol{\theta}_{\boldsymbol{max}}}$ and performing the examination test in Equation 7, the limited rotation transformation would be $\widetilde{\Delta\boldsymbol{c}}_{\boldsymbol{i}}^{\boldsymbol{t}''}$ and the final combined path description would be $\{\boldsymbol{T}_{\boldsymbol{C}}'''\}^{\boldsymbol{b}}$ (Equation 8).

$$\Delta\boldsymbol{c}^{r} = \Delta\boldsymbol{R}_{\boldsymbol{y},\boldsymbol{\theta}} \times \Delta\boldsymbol{R}_{\boldsymbol{z},\,\boldsymbol{\psi}} \qquad (5)$$

$$\Delta\mathrm{c}_i^{t''} = \left(\boldsymbol{T}_{\boldsymbol{C}_i}''^{\boldsymbol{b}}\right)^{-1} \times \boldsymbol{T}_{\boldsymbol{r}}^{\boldsymbol{b}} \times \Delta c_i^r \Rightarrow \Delta\boldsymbol{c}_i^{t''} = \boldsymbol{T}_{\boldsymbol{r}}^{\boldsymbol{b}} \times \Delta\boldsymbol{c}_i^r \times \boldsymbol{T}_{\boldsymbol{C}_i}''^{\boldsymbol{b}} \qquad (6)$$

$$\text{Test: } \begin{Bmatrix} \boldsymbol{IF}\ |\Delta\boldsymbol{R}_{\boldsymbol{z},\,\boldsymbol{\psi},\boldsymbol{i}}| > \Delta\boldsymbol{R}_{\boldsymbol{z},\,\boldsymbol{\psi}_{\boldsymbol{max}}} & \Rightarrow & \Delta\boldsymbol{R}_{\boldsymbol{z},\,\boldsymbol{\psi},\boldsymbol{i}} = (\pm)\,\Delta\boldsymbol{R}_{\boldsymbol{z},\,\boldsymbol{\psi}_{\boldsymbol{max}}} \\ \mathbf{IF}\ |\Delta\boldsymbol{R}_{\boldsymbol{y},\boldsymbol{\theta},\boldsymbol{i}}| > \Delta\boldsymbol{R}_{\boldsymbol{y},\boldsymbol{\theta}_{\boldsymbol{max}}} & \Rightarrow & \Delta\boldsymbol{R}_{\boldsymbol{y},\boldsymbol{\theta},\boldsymbol{i}} = (\pm)\,\Delta\boldsymbol{R}_{\boldsymbol{y},\boldsymbol{\theta}_{\boldsymbol{max}}} \end{Bmatrix} \Rightarrow \Delta\boldsymbol{c}_i^{t''} \to \widetilde{\Delta\boldsymbol{c}}_i^{t''} \qquad (7)$$

$$\{\boldsymbol{T}_{\boldsymbol{C}}'''\}^{\boldsymbol{b}} = \{\boldsymbol{T}_{\boldsymbol{C}}''\}^{\boldsymbol{b}} \times \{\widetilde{\Delta\boldsymbol{c}}\}^{t''} \qquad (8)$$

As shown above, several transformations need to be applied to achieve the collision-free trajectory in the complex groove geometry including planned multiple and related path definition, the operator modification during the online process and the continuous collision avoidance.

6 Experimental Verification

The proposed welding robot system is intended to replace manual welding methods by offering OLP and system wise process support. The performance of the system is compared to the manual metal arc welding procedure (which is the currently applied welding method for the examined manufacturing facility) and to online programming method. Each test case repeated for each of the three methods. The main properties for comparison of the different welding methods are 1) the total time spent on between the work-piece installation and final welding inspection, 2) time spent on the different tasks and their added value to the process, and 3) quality of the produced weld.

6.1 Experimental Setup

The robotic welding system design was implemented in a test robot cell for manufacturing Francis hydropower turbine runners. The robot cell was built up from an *OTC* FD-V20A high precision welding robot arm with 0.01 mm repetition accuracy, *FroniusMagicWave4000* welding power source including wire feeder unit and TIG welding torch, *PEMA 35 0000 FAS* manipulator unit, *Cavilux* welding camera system, together with additional safety and interfacing subsystems.

For the test setup, the base material of the runner was 1.4313 X3CrNiMo13-4 martensitic stainless steel. Argon 4.6 gas (purity over 99.996%) was used as the shielding gas with a constant14 l/min flow rate. For deposition, 1.2 mm diameter CN 13/4-IG filler wire was used, continuously fed to the base material that was preheated to 80 °C temperature. The working angle of the welding torch is fixed at 90 degrees to the work-piece.

The range of the welding parameters was defined during the pre-welding procedure qualification, where wider limits were established. The sets were selected to produce heat input between 0.8 kJ/mm and 1.2 kJ/mm using direct current electrode negative (DCEN) current flow. The weld beads were placed in three 30-degree bevel angle V grooves of two 20 mm thick plates on 400 mm length with a gap of 2 mm and a root face of 2 mm. The plan consisted of 37 weld beads of each three test grooves. Their distribution is shown in Figure 10a. The welded structure went through heat treatment to improve the base material's mechanical properties by quenching and tempering.

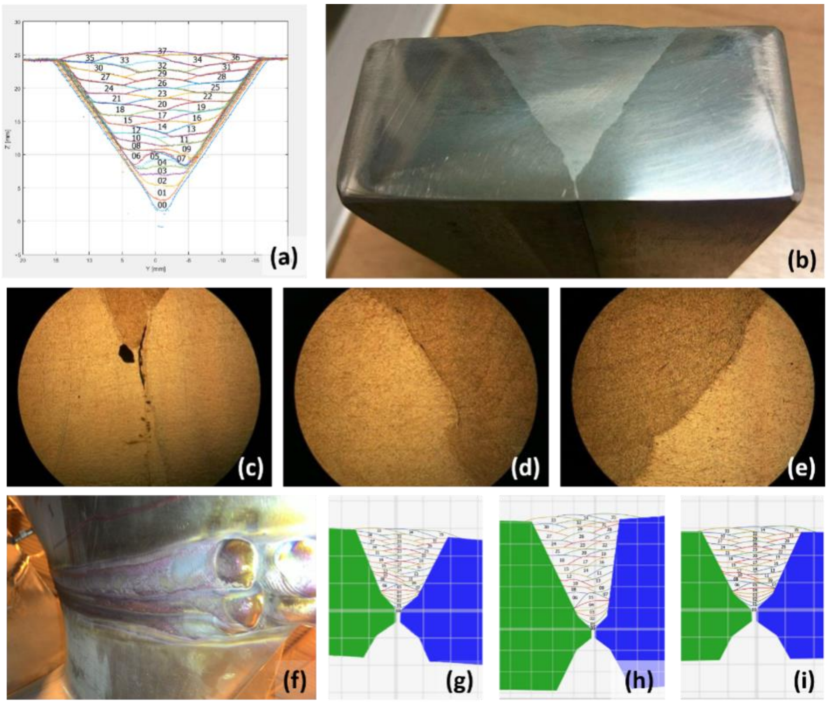

Figure 10
(a) Multi-pass weld bead placement pattern of the test work-piece, (b) prepared cross-section for macro etching, (c) impurity in the root of the weld, (d, e) merge on the height 6.4 mm on the left and right side, (f) filled seam on the runner of Francis hydropower turbine, (g, h, i) multi-pass weld bead placement pattern on the runner

The procedure of the experiments and their analysis followed the NS-EN ISO 15614-1 standard. The seams were examined by non-destructive methods such as penetrant testing, visual and ultrasonic inspection. After the stress relieving heat treatment, the test pieces were cut for destructive mechanical property testing for tensile, hardness and bend test. One of the cross-sections of the robot welded test work-piece is prepared for the macro etching, and the polished surface is shown in Figure 10b. The quality of the weld was examined under a microscope, were the root of the weld showed some impurity (Figure 10c), but the overall fusion found sufficient (Figure 10d-e). The exact test results of the mechanical property tests are not discussed due to industrial partner's restriction on data publication, but they were within the required range for each mechanical property and matched the base material's corresponding nominal values but outstanding excellent impact energy results. The welding parameter ranges defined during the welding procedure qualification test were the followings: arc voltage varies between 11 and 14 V, arc current is DCEN and ranges between 200 and

350 A, wire feed rate up to 200 cm/min, and welding speed ranges between 1.5 and 3.5 mm/s.

The runner of the Francis hydropower turbine assembled from 17 blades; the grooves are with double U edge preparation in the middle section of the blades on a 560 mm length. Base material thickness is between 10 and 40 mm and changing gradually along the groove. The predefined welding parameter windows were used in all the three welding test cases, and the weld quality was examined by the previously mentioned non-destructive methods. The filled seam of blades is shown in Figure 10f, and the planned cross-sectional weld bead patterns, in the positions, marked earlier in Figure 6 are presented in Figure 10g-i.

6.2 Evaluation of the Experiments

The baseline for the comparison defined by the total time spent on the manual metal arc welding, where the processing time divided between the welding (34%), grinding (20%) and resting time (46%), later due to the EHS requirements. The performances of the robotized methods are presented in Figure 11.

The online programmed robotic welding robot system (Online RWS) program introduced TIG welding and resulted in significant improvement in most parameters compared to the manual welding. The lead time reduced with 22.4% and the proportion of the welding and grinding tasks improved to 40% and 2%, respectively. The remaining time is utilized as online programming time instead of non-productive resting time.

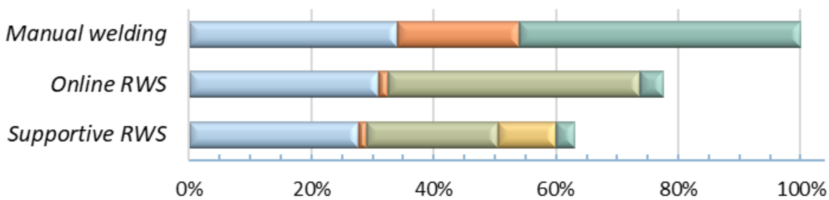

	Supportive RWS	Online RWS	Manual welding
Welding	27.8%	31.0%	34.0%
Grinding	1.3%	1.6%	20.0%
Verification	21.5%	41.1%	0.0%
Preparation	9.5%	0.0%	0.0%
Unproductive	3.2%	3.9%	46.0%

* values are realtive to the total time spent on Manual welding

Figure 11

Distribution of activity time spent on subtasks*

The supportive robotic welding system (Supportive RWS) further reduced the total process time by 18.7% compared to the Online RWS, requiring only 63.1% of the manual process total time. The proportion of welding (44%) and grinding (2%) time is similar the Online RWS, but the introduction of OLP reduced the online programming time significantly, being the main factor of process time improvement.

In manual welding, the time of the process is directly translated into the work-piece, and the gained experience during execution cannot be transmitted to the following work-pieces. Thus, the lead time and the welding quality highly depends on the welder's skills. More consistent quality is achieved by the Online RWS and the Supportive RWS, where the set of welding parameters were defined more precisely, but increased amount of welding defects was detected during the online programming method. Those defects were traced back to the misjudged positioning due to the work-piece limited accessibility and the curvature of the groove. With the Supportive RWS decreased number of welding defects was detected.

Conclusions

In this paper, a supportive robot system design for multi-pass welding was introduced, that can handle non-uniform grooves in small series production. The proposed system design is based on a welding process modelling method as simplified offline programming (OLP), and process execution to support interfacing. The key component of the welding process modelling method is the multi-pass welding planning complexity reduction from a three-dimensional into consecutive two-dimensional with dedicated consideration of the non-uniformities of the welding groove. The modelling is applying a mathematical description approach, executed on each reference cross-section. It feeds the multi-pass welding planning module, where the weld beads are planned to be deposited layer by layer and their shapes are also given in mathematical models to keeping their and the groove's curvatures as accurate as possible.

The online system segment of the proposed system design includes simulation synchronization with the welding process and a human-in-the-loop control method with supportive adjustment functions; where the first provides non-observable information to the operator. The reference cross-sections generated during OLP serves as a modification plane that remains constant to ensure the trackability of the modifications during the operation and to provide information to the later refinement of the multi-pass welding plan. Involving the human operator in the loop enables online quality control and process modification to ensure high final quality of the welding. The system design was implemented for a use case of a Francis hydropower turbine runner. The welding experiments showed that it could support the robot operator during the welding process and to handle the non-uniform grooves.

Acknowledgement

The research reported in this paper was partially supported by the Norwegian Research Council through the project 245691 “Cognitive robot welding system (CoRoWeld)” and the Industrial PhD project 244972/O30 “Virtual presence in remote operation of industrial robot”. Further partial support was given by the Higher Education Excellence Program of the Ministry of Human Capacities in the frame of TOPIC research area of Budapest University of Technology and Economics (BME FIKP-MI).

References

[1] B. M. Abdullah, A. Mason, A. Al-Shamma’a, Defect detection of the weld bead based on electromagnetic sensing, Journal of Physics: Conference Series. 450, pp. 12-39, 2013

[2] M. H. Ang, L. Wei, L. S. Yong, An industrial application of control of dynamic behavior of robots-a walk-through programmed welding robot, in: International Conference on Robotics and Automation, 2000

[3] G. Bolmsjö, M. Olsson, Sensors in robotic arc welding to support small series production, Industrial Robot: An International Journal. 32, 2005

[4] B. Daniel, P. Korondi, G. Sziebig, T. Thomessen, Evaluation of Flexible Graphical User Interface for Intuitive Human Robot Interactions, Acta Polytechnica Hungarica. 11, 2014

[5] D. R. Delapp, Observations of solidification and surface flow on autogenous gas tungsten arc weld pools., Ph.D. dissertation, Vanderbilt Univ., 2005

[6] H. C. Fang, S. K. Ong, A. Y. C. Nee, Adaptive pass planning and optimization for robotic welding of complex joints, Advances in Manufacturing. 5, 2017

[7] F. Ferraguti, C. T. Landi, C. Secchi, C. Fantuzzi, M. Nolli, M. Pesamosca, Walk-through Programming for Industrial Applications, Procedia Manufacturing. 11, pp. 31-38, 2017

[8] M. Franke, B.-C. Pirvu, D. Lappe, B.-C. Zamfirescu, M. Veigt, K. Klein, K. Hribernik, K.-D. Thoben, M. Loskyll, Interaction Mechanism of Humans in a Cyber-Physical Environment, in: Dynamics in Logistics, Springer, 2016

[9] M. Fridenfalk, Development of intelligent robot systems based on sensor control, Lund Univ., 2003

[10] T. Gabor, L. Belzner, M. Kiermeier, M. T. Beck, A. Neitz, A Simulation-Based Architecture for Smart Cyber-Physical Systems, in: International Conference on Autonomic Computing, IEEE, pp. 374-379, 2016

[11] P. Galambos, Vibrotactile feedback for haptics and telemanipulation: Survey, concept and experiment, Acta Polytechnica Hungarica. 9, 2012

[12] G. Gökmen, Y. Karatepe, T. Ç. Ak, M. Kurtulmu, Spectrum Analysis of GMA Welter in Various Working Modes, Acta Polytechnica Hungarica. 9, pp. 5-16, 2012

[13] W. P. Gu, Z. Y. Xiong, W. Wan, Autonomous seam acquisition and tracking system for multi-pass welding based on vision sensor, Int J Adv Manuf Technol. 69, pp. 451-460, 2013

[14] T. Haidegger, L. Kovács, R.-E. Precup, B. Benyó, Z. Benyó, S. Preitl, Simulation and control for telerobots in space medicine, Acta Astronautica. 81, pp. 390-402, 2012

[15] T. Hatano, C. M. Horvath, T. Thomessen, M. Niitsuma, A vibrotactile navigation aid for remote operation of an industrial robot, in: International Symposium on System Integration, IEEE/SICE, pp. 700-705, 2016

[16] C. M. Horváth, S. Kovács, New cognitive info-communication channels for human-machine interaction, Recent Innovations in Mechatronics. 4, 2017

[17] C. M. Horvath, T. Thomessen, P. Korondi, Robotized Multi-Pass Tungsten Inner Gas Welding of Francis Hydro Power Turbines, in: IEEE IES, Edinburgh, Scotland, United Kingdom, pp. 1759-1765, 2017

[18] E. Horváth, C. Pozna, R.-E. Precup, Robot Coverage Path Planning Based on Iterative Structured Orientation, Acta Polytechnica Hungarica. 15, pp. 231-249, 2018

[19] IFR, Executive Summary World Robotics 2017 Industrial Robots, 2017

[20] P. Kah, M. Shrestha, E. Hiltunen, J. Martikainen, Robotic arc welding sensors and programming in industrial applications, Int J Mech Mater Eng. 10, 2015

[21] H. C. E. Kjeldsen, Sensor Based Welding Automation Modelling System: Including a Specially Developed Low-cost Temp. Imaging System, 2007

[22] T. Kosicki, T. Thomessen, Cognitive Human-Machine Interface Applied in Remote Support for Industrial Robot Systems, International Journal of Advanced Robotic Systems. 10, pp. 342, 2013

[23] Y. Liu, W. Zhang, Y. Zhang, Dynamic Neuro-Fuzzy-Based Human Intelligence Modeling and Control in GTAW, IEEE Transactions on Automation Science and Engineering. 12, pp. 324-335, 2015

[24] Y. Liu, Y. Zhang, Toward Welding Robot With Human Knowledge: A Remotely-Controlled Approach, IEEE Transactions on Automation Science and Engineering. 12, pp. 769-774, 2015

[25] O. Madsen, C. Bro, M. B. Madsen, A Software module for planning of robotized multi-pass welding, in: 10th International Conference on Computer Technology in Welding and Manufacturing, Denmark, 2000

[26] J.A. Marvel, Collaborative Robots: A Gateway Into Factory Automation, ThomasNet News. 2014

[27] D. Massa, M. Callegari, C. Cristalli, Manual guidance for industrial robot programming, Industrial Robot: An International Journal. 42, 2015

[28] P. McGuire, J. Fritsch, J. J. Steil, F. Rothling, G. A. Fink, S. Wachsmuth, G. Sagerer, H. Ritter, Multi-modal human-machine communication for instructing robot grasping tasks, in: International Conference on Intelligent Robots and Systems, IEEE/RSJ, pp. 1082-1088, Vol. 2, 2002

[29] L. Monostori, Cyber-physical Production Systems: Roots, Expectations and R&D Challenges, Procedia CIRP. 17, pp. 9-13, 2014

[30] P. Muller, J. Julius, D. Herr, L. Koch, V. Peycheva, McKiernan, Sean, Ann. Report on European SMEs 2016/2017: Focus on self employment 2017

[31] A. Y. Nee, Handbook of Manufacturing Engineering and Technology Springer London, 2015

[32] E. Negri, L. Fumagalli, M. Macchi, A Review of the Roles of Digital Twin in CPS-based Production Systems, Procedia Manufacturing. 11, 2017

[33] A. D. Nicholson, Rapid adaptive programming using image data, Ph.D. dissertation, University of Wollongong, 2005

[34] Z. Pan, J. Polden, N. Larkin, S. Van Duin, J. Norrish, Recent progress on programming methods for industrial robots, Robotics and Computer-Integrated Manufacturing. 28, pp. 87-94, 2012

[35] S. Pieskä, J. Kaarela, O. Saukko, Towards easier human-robot interaction to help inexperienced operators in SMEs, in: 3rd International Conference on Cognitive Infocommunications, pp. 333-338, 2012

[36] J. N. Pires, A. Loureiro, G. Bolmsjö, Welding Robots: Technology, System Issues and Application Springer Science & Business Media, 2006

[37] J. N. Pires, A. Loureiro, T. Godinho, P. Ferreira, B. Fernando, J. Morgado, Welding robots, IEEE Robotics Automation Magazine. 10, 2003

[38] T. P. Quinn, C. Smith, C.. McCowan, E. Blachowiak, R.. Madigan, Arc sensing for defects in constant-voltage gas metal arc welding, Welding Journal. 78, pp. 322-328, 1999

[39] M. Riedl, H. Zipper, M. Meier, C. Diedrich, Cyber-physical systems alter automation architectures, Annual Reviews in Control. 38, 2014

[40] K. Samu, B. Thamó, Internet based light quality measurement, Recent Innovations in Mechatronics. 4, p. 5, 2017

[41] R. D. Schraft, C. Meyer, The Need For An Intuitive Teaching Method For Small And Medium Enterprises, in: Proceedings of the ISR-Robotik., Munich, Germany, p. 10, 2006

[42] B. Siciliano, L. Villani, Robot Force Control Springer Science & Business Media, 2012

[43] B. Solvang, G. Sziebig, P. Korondi, Robot Programming in Machining Operations, in: Robot Manipulators, Intechweb, pp. 479-496, 2008

[44] S. Sugita, T. Itaya, Y. Takeuchi, Development of robot teaching support devices to automate deburring and finishing works in casting, Int J Adv Manuf Technol. 23, pp. 183-189, 2004

[45] B. Takarics, P. T. Szemes, G. Nemeth, P. Korondi, Welding trajectory reconstruction based on the Intelligent Space concept, in: 2008 Conference on Human System Interactions, pp. 791-796, 2008

[46] F. Tao, J. Cheng, Q. Qi, M. Zhang, H. Zhang, F. Sui, Digital twin-driven product design, manufacturing and service with big data, The International Journal of Advanced Manufacturing Technology. 94, pp. 3563-3576, 2018

[47] T. Thomessen, M. Niitsuma, K. Suzuki, T. Hatano, H. Hashimoto, Towards Virtual Presence Based on Multimodal Man-Machine Communication: A Remote Operation Support System for Industrial Robots, IFAC-PapersOnLine. 48, pp. 172-177, 2015

[48] J. Wu, J.S. Smith, J. Lucas, Weld bead placement system for multipass welding, IEE Proc.-Science, Measurement and Technology. 143, 1996

[49] Y. Xu, N. Lv, G. Fang, S. Du, W. Zhao, Z. Ye, S. Chen, Welding seam tracking in robotic gas metal arc welding, J of Mat. Proc. Tech. 248, 2017

[50] Y. Xu, H. Yu, J. Zhong, T. Lin, S. Chen, Real-time seam tracking control technology during welding robot GTAW process based on passive vision sensor, Journal of Materials Processing Technology. 212, 2012

[51] S. Yan, H. Fang, S. Ong, A. Nee, Optimal pass planning for robotic welding of large-dimension joints with nonuniform grooves, Proceedings of the Institution of Mechanical Engineers, Part B: J. of Eng. Manufacture. 2017

[52] S. J. Yan, S .K. Ong, A. Y. C. Nee, Optimal Pass Planning for Robotic Welding of Large-dimension Joints with Deep Grooves, Procedia CIRP. 56, pp. 188-192, 2016

[53] H. Zhang, H. Lu, C. Cai, S. Chen, Robot Path Planning in Multi-pass Weaving Welding for Thick Plates, in: T.-J. Tarn, S.-B. Chen, G. Fang (Eds.), Robotic Welding, Intelligence and Automation, Springer Berlin Heidelberg, pp. 351-359, 2011

[54] W. J. Zhang, Y. M. Zhang, Dynamic Control of the GTAW Process Using a Human Welder Response Model, Welding Journal. 92, pp. 154-166, 2013

[55] Z. Zhang, H. Chen, Y. Xu, J. Zhong, N. Lv, S. Chen, Multisensor-based real-time quality monitoring by means of feature extraction, selection and

modeling for Al alloy in arc welding, Mechanical Systems and Signal Processing. 60, pp. 151-165, 2015

List of Symbols

$\boldsymbol{a}$	path normal vector at the task point
$\boldsymbol{b}$	robot's base coordinate system
$\underline{\mathrm{C}}$	task point coordinates
$\Delta\boldsymbol{c}^{\boldsymbol{r}}$	transformation for collision avoidance, relative to $\boldsymbol{r}$
$\Delta\boldsymbol{c}_{\boldsymbol{i}}^{\boldsymbol{t}''}$	transformation for collision avoidance, relative to $\boldsymbol{t}''$
$\widetilde{\Delta\boldsymbol{c}}_{\boldsymbol{i}}^{\boldsymbol{t}''}$	range limited transformation for collision avoidance, relative to $\boldsymbol{t}''$
$\boldsymbol{n}$	Path tangent vector at the task point
$\Delta\boldsymbol{p}^{\boldsymbol{t}}$	Translation modification at $\boldsymbol{t}$
$\boldsymbol{r}$	CAD/CAM model coordinate system
$\Delta\boldsymbol{r}^{\boldsymbol{t}'}$	rotation transformation applied on $\boldsymbol{t}'$
$\Delta\boldsymbol{R}_{\boldsymbol{x},\boldsymbol{\varphi}}$	user rotation around the x-axis of the task point
$\Delta\boldsymbol{R}_{\boldsymbol{y},\boldsymbol{\theta}}$	user rotation around the y-axis of the task point
$\Delta\boldsymbol{R}_{\boldsymbol{z},\boldsymbol{\psi}}$	user rotation around the z-axis of the task point
$\boldsymbol{s}$	third vector at the task point ($\boldsymbol{s} = \boldsymbol{a} \times \boldsymbol{n}$)
$\boldsymbol{t}$	local coordinate system at the task point
$\boldsymbol{t}'$	modified task point's coordinate system, only user translation, relative to $\boldsymbol{t}$
$\boldsymbol{t}''$	modified task point's coordinate system, only user rotation, relative to $\boldsymbol{t}'$
$\{\boldsymbol{T}_{\boldsymbol{C}}\}^{\boldsymbol{r}}$	task path description in $\boldsymbol{r}$
$\{\boldsymbol{T}_{\boldsymbol{C}}\}^{\boldsymbol{b}}$	task path description in $\boldsymbol{b}$
$\{\boldsymbol{T}'_{\boldsymbol{C}}\}^{\boldsymbol{b}}$	task path description in $\boldsymbol{b}$ after user translation modification
$\{\boldsymbol{T}''_{\boldsymbol{C}}\}^{\boldsymbol{b}}$	task path description in $\boldsymbol{b}$ after user rotation modification
$\{\boldsymbol{T}'''_{\boldsymbol{C}}\}^{\boldsymbol{b}}$	Final task path description in $\boldsymbol{b}$, including all modification combined
$\boldsymbol{T}_{\boldsymbol{r}}^{\boldsymbol{b}}$	transformation matrix from $\boldsymbol{r}$ to $\boldsymbol{b}$
φ	welding torch working angle,
θ	welding torch travel angle
ψ	rotation angle around the electrode main axis